Published in final edited form as:
J Biomed Mater Res A. 2010 July ; 94(1): 205–213. doi:10.1002/jbm.a.32659.

EFFECTS OF CYCLIC FLEXURAL FATIGUE ON PORCINE BIOPROSTHETIC HEART VALVE HETEROGRAFT BIOMATERIALS

Ali Mirnajafi, **Brett Zubiate**, and **Michael S. Sacks***
Engineered Tissue Mechanics and Mechanobiology Laboratory, Department of Bioengineering and the McGowan Institute, University of Pittsburgh, Pittsburgh, PA 15219

Abstract

While bioprosthetic heart valves (BHV) remain the primary treatment modality for adult heart valve replacement, continued problems with durability remain. Several studies have implicated flexure as a major damage mode in porcine-derived heterograft biomaterials used in BHV fabrication. While conventional accelerated wear testing can provide valuable insights into BHV damage phenomena, the constituent tissues are subjected to complex, time-varying deformation modes (i.e. tension and flexure), that do not allow for the control of the amount, direction, and location of flexure. Thus, in the present study customized fatigue testing devices were developed to subject circumferentially oriented porcine BHV tissue strips to controlled cyclic flexural loading. By using this approach, we were able to study layer-specific structural damage induced by cyclic flexural tensile and compressive stresses alone. 10×10^6, 25×10^6 and 50×10^6 cycle levels were used, with resulting changes in flexural stiffness and collagen structure assessed. Results indicated that flexural rigidity was markedly reduced after only 10×10^6 cycles, and progressively decayed at a lower rate with cycle number thereafter. Moreover, the against-curvature fatigue direction induced the most damage, suggesting that the ventricularis and fibrosa layers have low resistance to cyclic flexural compressive and tensile loads, respectively. The histological analyses indicated progressive collagen fiber delamination as early as 10×10^6 cycles, but otherwise no change in gross collagen orientation. Our results underscore that porcine-derived heterograft biomaterials are very sensitive to flexural fatigue, with delamination of the tissue layers the primary underlying mechanism. This appears to be in contrast to pericardial BHV, wherein high tensile stresses are considered to be the major cause of structural failure. These findings point towards the need for the development of chemical fixation technologies that minimize flexure induced damage to extend porcine heterograft biomaterial durability.

Keywords

heart valve bioprostheses; heterograft biomaterial fatigue; flexure

INTRODUCTION

Bioprosthetic heart valves (BHV) fabricated from biologically derived heterograft biomaterials continue to be the dominant replacement valve modality, either as a conventional prosthetic design or more recently for percutaneous delivery 1. Regardless of the specific design, long-term fatigue resilience remains major limitation in the durability of

*For correspondence: Michael S. Sacks, Ph. D., 100 Technology Drive, Room 234, University of Pittsburgh, Pittsburgh, PA 15219, Tel: 412-235-5146, Fax: 412-235-5160, msacks@pitt.edu

any device utilizing these biomaterials. Leaflet mineralization, with or without leaflet tearing 24, and mechanical fatigue 48, are two primary processes in limiting the porcine BHV life time. Fatigue damage independent of calcification has been shown to be a cause of structural damage to the leaflets of bioprostheses 9, indicating that tissue structural damage independent of calcification is mechanism of deterioration 6,9,12. Moreover, after chemical fixation the entire extracellular matrix is highly bonded, inducing a substantial increase in tissue stiffness in the low strain range 1,7,13,14, as well as essentially eliminating the ability for tissue fiber to slide relative to each other.

Given the long term clinical expectations for replacement heart valves (at least 15 patient years, or about 600 million cycles), BHV durability evaluations need to be conducted for over millions of cycles. This is accomplished in industrial settings using accelerated wear testing (AWT), wherein fully intact and functioning valves are subjected to hydrodynamically induced opening/closure cycles at rates 13–25 Hz. Pressure across the closed valve is maintained at a minimum of 90 mmHg for aortic valves and 120 mmHg for mitral valve implants. Generally, tissue valves are tested for 200 million cycles (the FDA recommend level, equivalent to 5 patient years), with the effects of tissue fatigue described after visual inspection at the end of the test 15. Using in-vitro AWT, studies have shown ~50% reduction of failure stress and a marked reduction of failure strain of the leaflets of porcine BHVs after 120×10^6 cycles 16,17. We have observed a substantial reduction in tissue extensibility and increasing collagen fiber disorganization after only 50×10^6 cycles 8,18, as well as a large loss of ultimate tensile strength after 200×10^6 cycles 12.

While some degree of mechanistic damage information can be obtained from the AWT tested valves 1, it is hard from these studies to determine specific effects of tensile or compressive stresses and their relation to structural damage to the leaflet. Early work by Broom performed in-vitro studies on progressive deterioration of porcine BHV due to cyclic loading 19,21. Although strips of tissue specimens were subjected to cyclic tension, they were also subjected to compression due to buckling. Progressive fracture of collagen bundles was observed only in the regions that were bent upon unloading, and peak cyclic tension load did not affect the deterioration pattern. These results suggested that tissue disruption was not dependent upon tensile stress, but rather compressive stresses during flexure. However the amount and the direction of flexure were not controlled nor quantified.

In the present study, we investigated flexure fatigue behavior of porcine BHV tissues utilizing specialized instrumentation in order to quantitatively determine the roles of tensile and compressive stresses on porcine BHV heterograft biomaterial fatigue. Two customized devices were developed to apply pure cyclic flexural load to the prepared strips dissected from the belly region of porcine BHV in two directions of fatigue with in natural curvature (FW) or fatigue against natural curvature (FA) separately (Fig. 1), allowing for structural damage of the tissue layers to be isolated. To assess the mechanical effects effective flexural rigidity of specimens due to the fatigue was quantified using three point bending 5,22, with the specimens flexed within natural curvature (WC) and against natural curvature (AC). Structural damage was determined using small angle scattering light (SALS) 23,24 and conventional histology.

METHODS

Specimen preparation and test methodology

A total of 40 samples, 25 mm × 5 mm × 0.6 mm each, were dissected from the cuspal belly area (Fig. 1) of all three cusps of 4 mmHg glutaraldehyde fixed of 14 porcine BHV the courtesy of St. Jude Medical (St Jude Medical, MN). While leaflets consist of three distinct layers25,26, recent evidence suggests that the spongiosa layer may be considered

functionally a specialization of the inner portions of fibrosa and ventricularis 27. Also, since chemical fixation tightly binds the tissue layers, we regarded the porcine BHV leaflet as being composed of two structurally significant layers, the fibrosa and ventricularis, and treated the spongiosa as specialization of the inner portion of these layers. In order to subject fibrosa and ventricularis to cyclic compression and tension (Fig. 1-b), specimens were divided into the following two groups (Fig. 1-b):

1. Flex-fatigued in the direction of natural circumferential cuspal curvature (FW)
2. Flex-fatigued against the natural circumferential cuspal curvature (FA).

16 specimens from each group were subjected to cyclic flexural loading, with 4 additional specimens kept in the bath of the device unloaded as control. Specimens of both groups were subjected to 10×10^6, 25×10^6, and 50×10^6 cycles of flexural loading. These choices for cycle level were based on our previous studies that indicated that a major portion of structural damage to heterograft biomaterials occurs in the first 50×10^6 cycles 1،7،28،29, and thus provide the best starting place for mechanistic studies.

Device design

Two custom testing devices utilized were developed for this study to apply cyclic flexural loading. One device applied unidirectional load and the other one subjected specimen to bidirectional flexural cyclic loading. The device has the following two main components (Fig. 2). First, a computer-controlled actuator (ELF 3200, EnduraTEC Systems Corp., Minnetonka, MN, for FA device; a customized reciprocating unit for FW device), supplied the cyclic motion and was capable of producing a total displacement of approximately 0.75 inch at 35Hz. Secondly, a testing frame, which transferred the linear motion of actuator into pure flexure in specimens mounted in its grips. A heated bath recirculator (Model 1104, VWR International, South Plainfield, NJ) was used to supply a flow rate of 0.5 L/min of 0.9% phosphate buffered saline through a micro-filtration system and maintain the temperature at 37 °C.

For the FA-direction, specimens are initially slightly curved in the opposite direction, and then are flexed in the opposite direction, requiring the grips to initially move away then towards each other (Fig. 3a). A mechanism was designed to accommodate this motion for each loading unit with minimal vibration (Fig-2), and was able to test sixteen specimens. The device symmetry aided in balance to allow for a 20 Hz to 35 Hz operating range. A PVC strip allowed the desired rotation of grips based on the reciprocation of the circular plate to induce flexure without any direct contact other than the grips (Fig-3a). Specific peak curvatures were achieved by controlling the exposed length of the PVC, the specimen length, and the actuator displacement (Fig-3b). The FW device was simpler in design, with the grips attached around perimeter of two circular plates - one was stationary and another one is attached to a reciprocating shaft. Once these parameters are determined at the desired frequency, all specimens are loaded with the same values to produce the same changes of curvature.

Curvature estimation

Reference state of the specimens was obtained by imaging the front specimens while the device stopped at the reference state. Next, the device was started and run at 10 Hz, and a 10-second movie clip, with a stroboscope utilized isolate the specimen motion (Fig- 3a). Single frames showing the minimum, maximum, and reference curvatures were extracted from the movies and processed utilizing Sigmascan (Jandel Scientific Software, San Rafael, CA). This process was repeated at 15 Hz, 20 Hz, 25 Hz, and 30 Hz to estimate curvature change and axial strain at each speed.

Coordinates of the markers were digitized and the following quadratic equations was used to fit to the marker positions using least-squares regression,

$$y=ax^2+bx+c \quad (1)$$

The change in curvature Δκ of the specimen at each position was estimated using the second derivative of eqn. 1, and subtracting the curvature of flexed state from the curvature of resting state. The calculated change of curvature was compared with the physiological condition that we measured and reported in the past by testing a porcine BHV in-vitro 30. Note too that specimen geometry was checked regularly during the test to insure consistency during the testing period.

Strain measurement

In order to be sure that specimens were subjected to pure flexure during the test, maximum extentional strain during the test was calculated using

$$\varepsilon=\frac{(L_F - L_u)}{L_u} \times 100\% \quad (2)$$

where L_f is the length of the specimen at maximum flexure and L_u is the length of the specimen at resting state. A customized program was written to calculate both L_f and L_u using a cubic spline. In preliminary tests using phantoms of known length, lengths were determined to less than 1.0% error.

Determination of flexural rigidity

In order to estimate the changes of flexural rigidity due to the fatigue a 3-point bending test was used 5. In brief specimens were mounted in a custom made device and flexed in both directions of within natural curvature (WC) and against natural curvature (AC) and their change of curvature and flexing moment were measured. The moment M was applied to the specimen using calibrated bending bar, with the specimen instantaneous flexural rigidity EI was calculated from the Euler-Bernoulli relationship 31 $M = E(\Delta\kappa)I\ \Delta\kappa$, where Δκ is the current change in curvature, and I is the second moment of inertia. Note that we write $E= E(\Delta\kappa)$ to underscore the fact that this E is an function of the specimen's current Δκ and will in general change with increasing Δκ.

Assessment of the structural damage due to the fatigue

In order to quantify the structural damage due to cyclic loading, collagen fiber orientation of specimens were measured using small angle light scattering (SALS)24. In brief, SALS consist of passing He-Ne laser light through specimens and measuring the resultant scattered light distribution, which characterized the local collagen fiber architecture 32. One specimen after each cycle of loading plus one control specimen from each group (on total eight specimens) were examined using SALS. In addition, histological sections were prepared from selected test specimens after performing SALS. The specimens were paraffin-embedded and then sectioned at 10 μm thickness every 25 μm throughout the entire width. The embedded histological sections were incubated for 90 minutes on 0.1 % Sirius red F3BA (Polyscience Inc.) in saturated picric acid, rinsed in 0.01 *N* HCL. The sections then were dehydrated in graded ethanol solutions and put under cover slips. The sections were imaged under a light conventional microscope with magnification of 15X.

Statistical analysis

Statistical analysis (analysis of variance) was performed on the mean and standard error of the mean (SEM) values from both FA and FW groups and controls at all of cyclic loading increments with SigmaStat (Systat Software, San Jose, CA). Statistical significance was determined by p values of <0.05.

RESULTS

Estimation of the maximum Δκ and maximum strain during cyclic loading

The mean ± s.e.m of the maximum Δκ was 0.0992 ± 0.0009 mm^{-1}, consistent with the mean change of curvature of porcine BHV measured in-vitro of ~0.1 mm^{-1} 30. The maximum strain was 1.9±0.3% and occurred at the midpoint of the actuation cycle where the actuator is moving with the highest velocity (Fig. 3). Given the very small strain values, the device demonstrated its ability to provide controlled nearly pure cyclic flexure up to 35 Hz with desired changes in curvature similar to actual condition of functioning BHV.

The M-Δκ response

As in our previous AWT studies 1, the zero cycle specimens demonstrated a linear response (Fig. 4-a), with the AC direction about twice as stiff as the WC direction (Fig. 4-b). Generally, the relation became increasing non-linear with increasing number of cycles. Thus, to facilitate comparisons between test groups under similar mechanical states, EI values were calculated at instantaneous Δκ of 0.1 mm^{-1} , the mean change of curvature of porcine BHV in-vitro 30

Effects of fatigue

The flexural rigidity of specimens in AC direction of flexure decreased dramatically in the first 10×10^6 cycles for both the FA and FW groups (Fig. 5-a). After 10×10^6 cycle, flexural rigidity in AC direction decreased from 115.20 to 55.47 in FA group and from 101.97 kPa-mm^4 to 67.67 kPa-mm^4 in FW group (Fig. 5-a). The decrease of flexural rigidity became more gradual in both FA and FW groups after 25×10^6, and 50×10^6 cycles of loads (Fig. 5a). In AC direction, the flexural rigidity decreased only from 55.47 to 40.80 and 30.80 kPa-mm^4 for FA group and from 67.67 to 67.31 and 53.78 kPa-mm^4 for FW group at each increment of cyclic loading. Flexural rigidity in WC direction decreased slightly only on FA group and no alteration was observed in FW group, with the flexural rigidity among four groups statistically different only in FA group and only in AC direction. Note that no changes were observed over the same cycle time for the controls.

Effects of direction of cyclic loading on EI

Both groups exhibited a decrease in EI, with the FA group exhibiting a greater change in both AC and WC directions of flexure. Specifically, the FW group flexural rigidity in the AC direction slightly changed and in WC direction did not (Fig. 5-a). In AC direction of flexure, the flexural rigidity for FA group decreased over the cycle period 115.20 to 30.09 kPa-mm^4, while for FW group decreased 101.97 to 53.78 kPa-mm^4 over the cycle period. In WC direction of flexure, the decreases were for the FA group was 63.51 to 16.98 kPa-mm^4, while for FW group the flexural rigidity decreased 37.23 to 26.02 kPa-mm^4. To highlight these changes, we determined the relative changes in EI from their respective 0 cycle values which demonstrated that the FA group experienced approximately twice the drop in EI compared to the FW groups, with the AC testing direction experiencing the largest decreases in both groups (Fig. 5-b).

Structural changes

No pronounced change of fiber orientation was observed in either of groups after cyclic loading (Fig. 6). While a slight decrease of orientation index was observed only in 50×10^6 million cycles, it was not statistically significant. Histology demonstrated structural damage to the tissue, which was observed in all loading cycles for all specimens (Fig. 6). The structural damage was observed for both FA and FW groups. The area was subjected to the highest flexure during cyclic loading experienced the most severe damage.

DISCUSSION

BHV fabricated from heterograft biomaterials will continue to be extensively used and remain as the dominant replacement heart valve design for the coming several decades. Moreover, as third world countries continue to develop their medical infrastructure, worldwide valve replacement will continue to rise. Further, novel approaches to valve implantation, such as percutaneous valve technologies, are an alternative for patients in need of replacement heart valves that cannot undergo valve replacement surgery. These designs will require even more from their constituent materials due to the compaction of the valve required for implantation. Heterograft biomaterials will thus continue to be extensively used, so that rational, scientifically-based approaches to BHV biomaterial development and design will be required to significantly improved durability.

In the long history of BHV development various mechanisms for their limited durability have been implicated 33, including site-specific structural damage resulting from mechanical fatigue alone 9. As stated earlier, AWT can provide useful information on how the tissues behave in a functional valve. Using AWT, we have reported that BHV flexural rigidity dropped to half its initial value after 100×10^6 cycles 11 30. However, AWT cannot be used for more intensive studies of the specific mechanisms (especially those mechanical in nature) most responsible for tissue damage due to the highly complex nature of valve leaflet deformations over the cardiac cycle. Thus, in the present study on porcine heterograft biomaterials, we focused on *flexure-induced fatigue* due to its implication as the primary source of porcine BHV tissue breakdown using novel experimental approaches to produce highly controlled isolated flexural deformation modes. This approach was taken as part of our approach to determine which deformation mode induces the greatest damage. While there have been attempts to perform related studies 20،34،35, none have been able to study isolated flexure. We demonstrated that cyclic flex-fatigue alone induced a pronounced reduction in flexural rigidity that was dependent on bending direction. Moreover, structural results (Figs. 6 and 7) indicated that under flexure the central tissue layers become delaminated, but the constituent fibers were not fractured and retained their alignment. Taken as a whole, our results support the working hypothesis of the role of flexural deformations as the leading source of porcine BHV mechanically induced fatigue damage.

Effects of cyclic compression and cyclic tension on individual layer damage

Since valvular tissues are heterogeneous structures consisting of different layers with different properties, we conducted bi-directional flexure tests to gain insight into the functional changes to each layer. Specifically, by flexing specimens in opposite directions of AC and WC, the net effects of different layer moduli, different moduli in tension and compression within the same layer, and potential nonlinearity of M-ΔK in the specimen could be revealed. An advantage of the current study design was that the ventricularis of FA specimen group was subjected only to cyclic compressive load and fibrosa to primarily to tensile loads. Conversely in FW group ventricularis was subjected only to tensile cyclic load while fibrosa was exposed to only cyclic compression. We found that the flexural rigidity of FA group in AC direction experienced the greatest decrease in flexural rigidity. This

suggests that the ventricularis and fibrosa layers have low resistance to cyclic flexural compressive and tensile loads, respectively.

However, we emphasize that while directional fatigue effects were found, they were of a secondary nature. Overall, it is the inability of the cross-linked collagenous valvular ECM to withstand flexural deformations in general that contributes to the delamination and related fatigue effects. While perhaps not immediately affecting valvular performance, delamination could potentially allow for the macrophages, plasma proteins, and other blood components to enter the valve material, potentially initiating the calcification process 36. Regardless of the exact mechanism(s) involved, any breakdown of the BHV constituent materials will have a deleterious effect on BHV durability.

Limitations of the current study

Interactions of the specimen with the solution used in the tester during the study while running in higher frequency caused a lag between flexure of the grips and the specimen and should be carefully watched and monitored. This lag is a function of the frequency of cyclic loading, the viscosity of the utilized saline solution, and the area of the contact of the specimen with the solution. Moreover the maximum frequency that can be reached is limited and depends on the above mentioned factors. Since our focus was mechanical damage alone, we did not attempt to simultaneously induce calcification through changes in solution chemistry as performed by Glasmacher 37,38. However, the current device configuration does allow for this possibility. Finally it should be noted that the flexural rigidity calculated using the Euler-Bernoulli equation (Eqn. 7) represents the effective rigidity only for that particular direction at the specific $\Delta\kappa$ value, so that finite elastic approaches will be required for more complete descriptors of tissue behavior39.

Summary of findings and implications

In the native valve leaflet, the spongiosa layer contains a high concentration of glycosaminoglycans (GAGs) 40. GAGs have long been associated with the viscoelastic behavior of soft tissues, especially in the energy during cyclic deformations 41. Moreover, Vyavahare et al. have indicated that GAGs leach out under conditions of accelerated wear in as little as 10×10^6 cycles 7, consistent with the fatigue behavior in the current study. Recent work by Vyavahare et al. 14,42 and Connolly et al. 13 point the way to novel approaches in chemical modification that show promise in minimizing these effects. Taken as a whole, our findings have the following implications to porcine heterograft biomaterials:

1. The major mechanism of early to mid-level damage (up to 50 million cycles) is delamination. This is in contrary with findings of other studies that suggest fiber breakage, uncrimping, etc. as the major mechanism of the damage5,21,35,43,45.
2. Cyclic flexure damage occurs within the first 10×10^6 cycles, so that chemical modifications that minimize inter-layer bonding and/or are more compliant 13,46,48 may reduce this effect.
3. Chemical modifications that retain GAGs may also help13,14,42, although the exact nature of the role of GAGs in cross-linked BHV tissues remains to be elucidated.

Acknowledgments

This research was supported by NIH grants HL-063026 and HL-070969. The authors also thank St Jude Medical for providing specimens, and Jeremy Raymer and Leigh McClure for their help in collecting and data analysis.

REFERENCES

1. Sacks MS, Mirnajafi A, Sun W, Schmidt P. Bioprosthetic heart valve heterograft biomaterials: Structure, mechanical behavior and computational simulation. Expert Rev Med Devices. 2006; 3(6): 817–34. [PubMed: 17280546]
2. Schoen, FJ.; Levy, RJ.; Bodnar, E.; Frater, RWM. Replacement cardiac valves. Pergamon Press, Inc.; New York: 1991. Calcification of bioprosthetic heart valves; p. 125-148.
3. Schoen F, Levy R. Tissue heart valves: Current challenges and future research perspectives. Journal of Biomedical Materials Research. 1999; 47:439–465. [PubMed: 10497280]
4. Schoen F, Levy R. Pathology of substitute heart valves. Journal of Cardiac Surgery. 1994; 9:222–227. [PubMed: 8186572]
5. Gloeckner DC, Billiar KL, Sacks MS. Effects of mechanical fatigue on the bending properties of the porcine bioprosthetic heart valve. Asaio J. 1999; 45(1):59–63. [PubMed: 9952009]
6. Sacks, MS.; Schoen, FJ. Calcification-independent collagen damage in explanted clinical bioprosthetic heart valves. Society for Biomaterials; Providence, Rhode Island: 1999.
7. Vyavahare N, Ogle M, Schoen FJ, Zand R, GLoeckner DC, Sacks MS, Levy RJ. Mechanisms of bioprosthetic heart valve failure: Fatigue causes collagen denaturation and glycosaminoglycan loss. Journal of Biomedical Materials Research. 1999; 46:44–50. [PubMed: 10357134]
8. Wells SM, Sellaro T, Sacks MS. Cyclic loading response of bioprosthetic heart valves: Effects of fixation stress state on the collagen fiber architecture. Biomaterials. 2005; 26(15):2611–9. [PubMed: 15585264]
9. Sacks MS, Schoen FJ. Collagen fiber disruption occurs independent of calcification in clinically explanted bioprosthetic heart valves. J Biomed Mater Res. 2002; 62(3):359–71. [PubMed: 12209921]
10. Ferrans V, Spray T, Billingham M, Roberts W. Structural changes in glutaraldehyde-treated porcine heterografts used as substitute cardiac valves. American Journal of Cardiology. 1978; 41:1159–1184. [PubMed: 96684]
11. Sacks MS, Liao J, Schmidt D. Fiber recruitment models for heart valve tissues. Journal of Biomechanical Engineering. submitted.
12. Sacks MS. The biomechanical effects of fatigue on the porcine bioprosthetic heart valve. Journal of long-term effects of medical implants. 2001; 11(3&4):231–247. [PubMed: 11921666]
13. Connolly JM, Alferiev I, Clark-Gruel JN, Eidelman N, Sacks M, Palmatory E, Kronsteiner A, Defelice S, Xu J, Ohri R, Narula N, Vyavahare N, Levy RJ. Triglycidylamine crosslinking of porcine aortic valve cusps or bovine pericardium results in improved biocompatibility, biomechanics, and calcification resistance: Chemical and biological mechanisms. Am J Pathol. 2005; 166(1):1–13. [PubMed: 15631995]
14. Lovekamp JJ, Simionescu DT, Mercuri JJ, Zubiate B, Sacks MS, Vyavahare NR. Stability and function of glycosaminoglycans in porcine bioprosthetic heart valves. Biomaterials. 2006; 27(8): 1507–18. [PubMed: 16144707]
15. Prosthetic Devices Branch. D. o. C.. Respiratory and Neurological Devices. Replacement heart valve guidance. Center for Devices and Radiological Health (FDA); Rockfied, Maryland: 1993.
16. Vesely I, Barber JE, Ratliff NB. Tissue damage and calcification may be independent mechanisms of bioprosthetic heart valve failure. J Heart Valve Dis. 2001; 10(4):471–7. [PubMed: 11499593]
17. Purinya B, Kasyanov V, Volkolakov J, Latsis R, Tetere G. Biomechanical and structural properties of the explanted bioprosthetic valve leaflets. J Biomech. 1994; 27(1):1–11. [PubMed: 8106530]
18. Wells SM. Mechanical design of elastic biopolymers. Physics in Canada. 2003; 59(2):67–74.
19. Broom ND. Fatigue-induced damage in gluteraldehyde-preserved heart valve tissue. Journal of Thoracic and Cardiovascular Surgery. 1978; 76(2):202–211. [PubMed: 98672]
20. Broom ND. The stress/strain and fatigue behaviour of glutaraldehyde preserved heart-valve tissue. Journal of Biomechanics. 1977; 10:707–724. [PubMed: 415062]
21. Broom ND. An ‘in vitro’ study of mechanical fatigue in glutaraldehyde-treated porcine aortic valve tissue. Biomaterials. 1980; 1(1):3–8. [PubMed: 6781550]

22. Engelmayr GC Jr. Hildebrand DK, Sutherland FW, Mayer JE Jr. Sacks MS. A novel bioreactor for the dynamic flexural stimulation of tissue engineered heart valve biomaterials. Biomaterials. 2003; 24(14):2523–32. [PubMed: 12695079]
23. Sacks MS. Focus on materials with scattered light. Reserach & Development. September.1988 : 75–78.
24. Sacks MS, Smith DB, Hiester ED. A small angle light scattering device for planar connective tissue microstructural analysis. Ann Biomed Eng. 1997; 25(4):678–89. [PubMed: 9236980]
25. Thubrikar, M. The aortic valve. CRC; Boca Raton: 1990.
26. Sacks MS, Yoganathan AP. Heart valve function: A biomechanical perspective. Philos Trans R Soc Lond B Biol Sci. 2008; 363(1502):2481.
27. Stella JA, Sacks MS. On the biaxial mechanical properties of the layers of the aortic valve leaflet. J Biomech Eng. 2007; 129(5):757–66. [PubMed: 17887902]
28. Sellaro TL, Hildebrand D, Lu Q, Vyavahare N, Scott M, Sacks MS. Effects of collagen fiber orientation on the response of biologically derived soft tissue biomaterials to cyclic loading. J Biomed Mater Res A. 2007; 80(1):194–205. [PubMed: 17041913]
29. Sun W, Sacks M, Fulchiero G, Lovekamp J, Vyavahare N, Scott M. Response of heterograft heart valve biomaterials to moderate cyclic loading. J Biomed Mater Res. 2004; 69A(4):658–69.
30. Sugimoto H, Sacks MS. The effects of leaflet stiffness on the dynamic geometry of the bioprosthetic aortic heart valve. Annals of Biomedical Engineering. submitted.
31. Frisch-Fay, R. Flexible bars. Butterworths; Washington,DC: 1962.
32. Sacks MS, Chuong CJ, More R. Collagen fiber architecture of bovine pericardium. Asaio. 1994; 40:M632–637.
33. Schoen FJ. New frontiers in the pathology and therapy of heart valve disease: 2006 society for cardiovascular pathology, distinguished achievement award lecture, united states-canadian academy of pathology, atlanta, ga, february 12, 2006. Cardiovasc Pathol. 2006; 15(5):271–9. [PubMed: 16979034]
34. Broom N. Simultaneous morphological and stress-strain studies of the fibrous components in the wet heart valve leaflet tissue. Connective Tissue Research. 1978; 6:37–50. [PubMed: 149648]
35. Broom N. Fatigue-induced damage in glutaraldehyde preserved heart valve tissue. Journal of Cardiovascular Surgery. 1978; 76:202–211.
36. Schoen FJ, Levy RJ. Calcification of tissue heart valve substitutes: Progress toward understanding and prevention. Ann Thorac Surg. 2005; 79(3):1072–80. [PubMed: 15734452]
37. Glasmacher B, Deiwick M, Reul H, Knesch H, Keus D, Rau G. A new in vitro test method for calcification of bioprosthetic heart valves. Int J Artif Organs. 1997; 20(5):267–71. [PubMed: 9209927]
38. Glasmacher-Seiler B, Reul H, Rau G. In vitro evaluation of the calcification behavior of polyurethane biomaterials for cardiovascular applications. Journal of Long-Term Effects of Medical Implants. 1992; 2:113–126. [PubMed: 10171618]
39. Schmidt DE, Merryman WD, Sacks MS. In situ estimation of extracellular matrix stiffness-interstitial cell mechanical coupling in the aortic heart valve leaflet. Annals of Biomedical Engineering. submitted.
40. Schoen F. Aortic valve structure-function correlations: Role of elastic fibers no longer a stretch of the imagination. Journal of Heart Valve Disease. 1997; 6:1–6. [PubMed: 9044068]
41. Fung, YC. Biomechanics: Mechanical properties of living tissues. Springer Verlag; New York: 1993.
42. Lovekamp J, Vyavahare N. Periodate-mediated glycosaminoglycan stabilization in bioprosthetic heart valves. J Biomed Mater Res. 2001; 56(4):478–86. [PubMed: 11400125]
43. Billiar, K.; Sacks, M. Long-term mechanical fatigue response of porcine bioprosthetic heart valves; IMECEX 98; Anaheim, CA, ASME. 1998;
44. Christie GW, Gross JF, Eberhardt CE. Fatigue-induced changes to the biaxial mechanical properties of glutaraldehyde-fixed porcine aortic valve leaflets. Semin Thorac Cardiovasc Surg. 1999; 11(4 Suppl 1):201–5. [PubMed: 10660193]

45. Smith, DB. Biomedical Engineering. University of Miami; Miami: 1996. The effects of in-vitro accelerated testing on the porcine bioprosthetic heart valve; p. 78

46. Sacks MS, Hamamoto H, Connolly JM, Gorman RC, Gorman JH 3rd, Levy RJ. In vivo biomechanical assessment of trigycidylamine crosslinked pericardium. Biomaterials. 2007

47. Rapoport HS, Connolly JM, Fulmer J, Dai N, Murti BH, Gorman RC, Gorman JH, Alferiev I, Levy RJ. Mechanisms of the in vivo inhibition of calcification of bioprosthetic porcine aortic valve cusps and aortic wall with triglycidylamine/mercapto bisphosphonate. Biomaterials. 2007; 28(4): 690–9. [PubMed: 17027944]

48. Alferiev IS, Connolly JM, Levy RJ. A novel mercapto-bisphosphonate as an efficient anticalcification agent for bioprosthetic tissues. Journal of Organometallic Chemistry. 2005; 690:2543–2547.

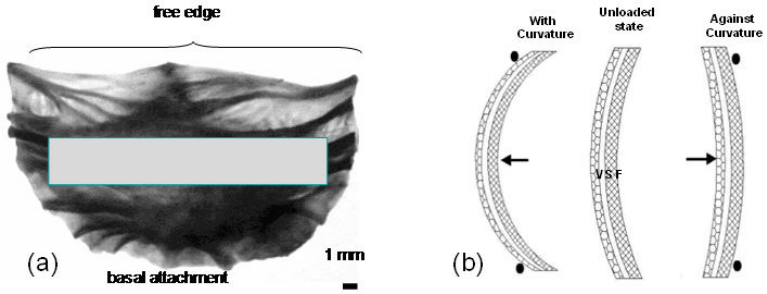

Fig. 1.
(a) The region of the leaflet from which the specimens were dissected, (b) a schematic highlighting how the leaflet layers are loaded under flexure.

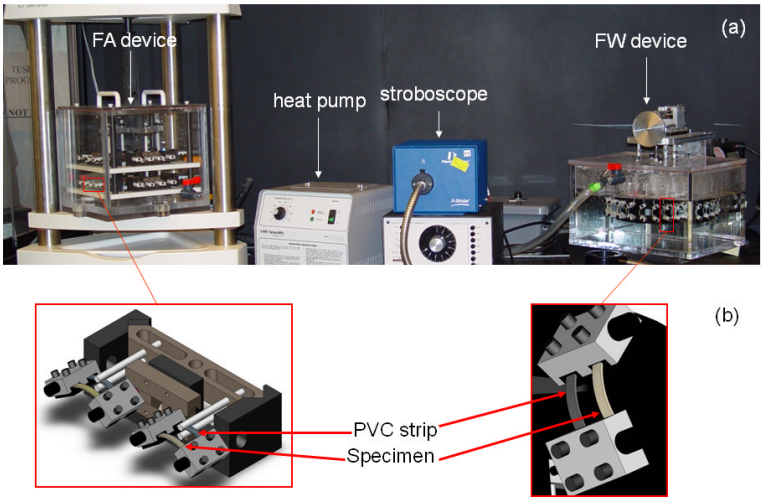

Fig. 2.
(a) A photo of the FA and FW fatigue devices and the overall experimental setup, and (b) enlarged schematic of the flexing mechanism.

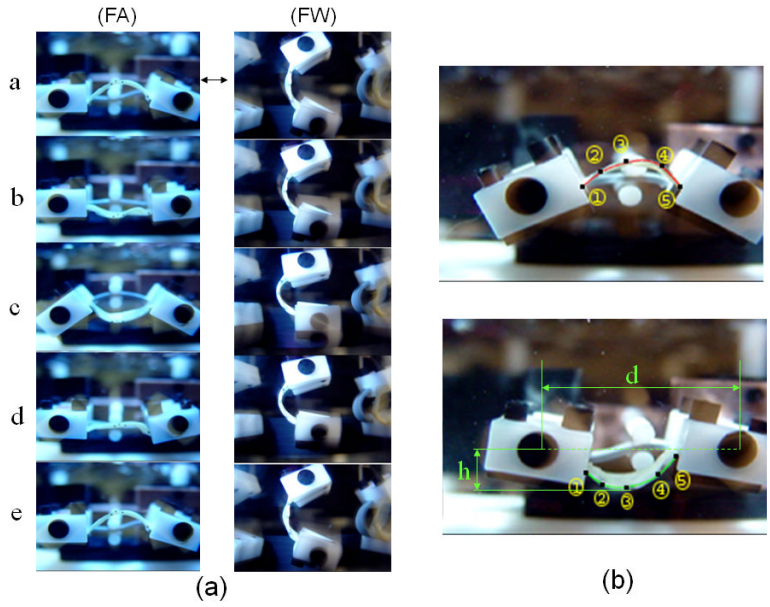

Fig. 3.

(a) Sequence of images representing a complete cycle of motion, (b) enlarged images depicting the extreme curvatures with numerical approximations of the sample shape superimposed. Here, the numbers indicate the marker number, d the pivot distance, and h the maximum specimen displacement. Instantaneous curvatures were determined by fitting the marker positions (see text for details).

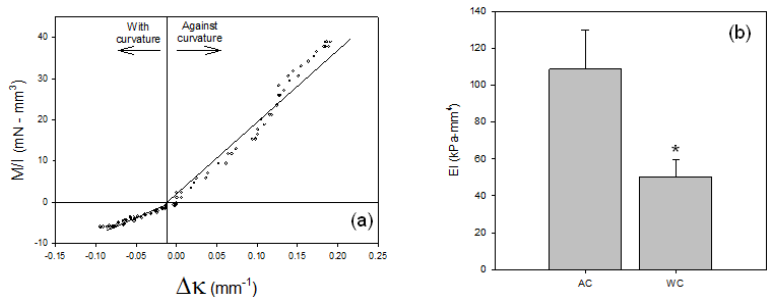

Fig. 4.

(a) Representative M/I-Δκ response for the BHV porcine tissues, highlighting the directional differences. The directional differences were consistent in all specimens, with approximately a 2:1 ratio between the AC and WC directions, respectively (b), clearly underscoring the effects of varying layer mechanical behaviors in the unicycle state. *-statistically significant ($p<0.05$) from the AC value.

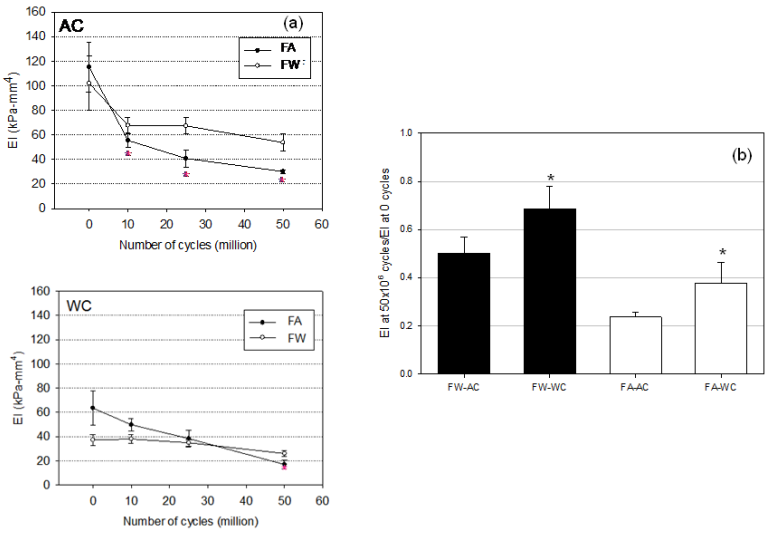

Fig. 5.

The flexural rigidity EI *vs.* cycle number for both FA and FW groups tested in both AC and WC directions. Both groups for both directions demonstrated substantial drop in EI with increasing cycle number, with the greatest changes occurring in the first 10×10^6 cycles. Normalized EI reductions indicated that the AC direction, regardless of the direction of applied cyclic flexure, experienced the greatest decrease in value. *-statistically significant ($p<0.05$) from the corresponding AC value.

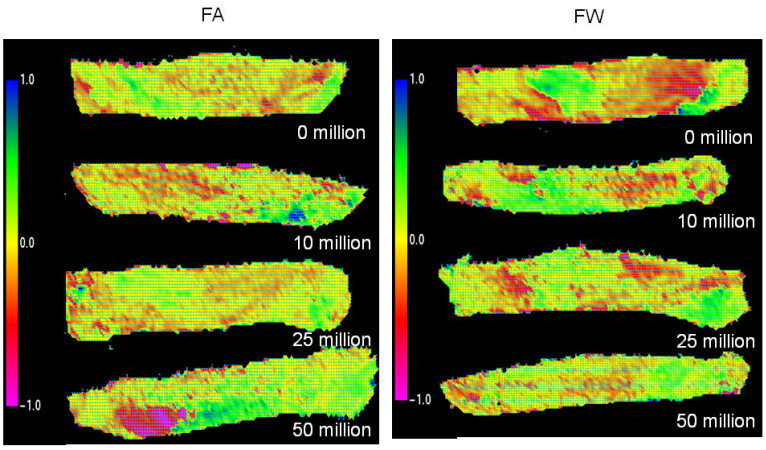

Fig. 6.
The results of SALS analysis of specimen from both FA and FW group scanned after each loading increment, indicating little change in overall collagen fiber alignment.

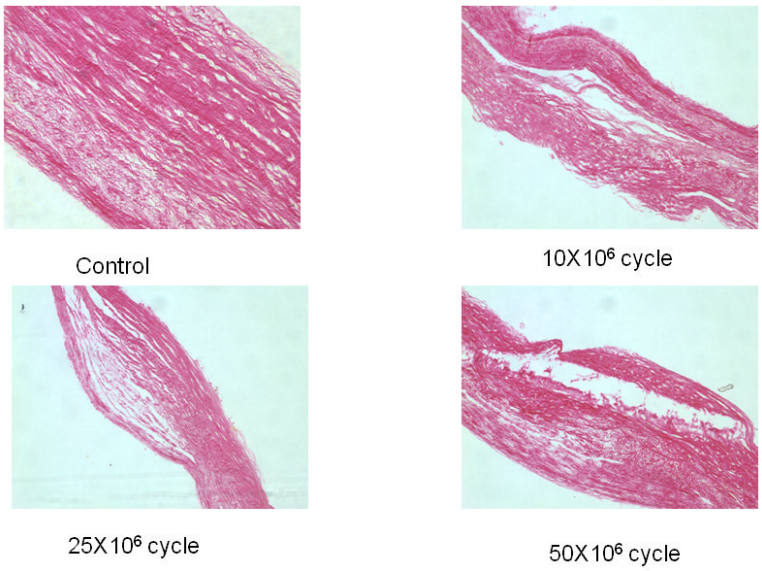

Fig. 7.
Results of histology of specimen of FA group analyzed after each loading cycle showing the complete cross section of the specimens. Note that progressive delamination occurred with increasing cycle number.